Mineralogical Magazine, August 2012, Vol. 76(4), pp. 851–861

Alcaparrosaite, $K_3Ti^{4+}Fe^{3+}(SO_4)_4O(H_2O)_2$, a new hydrophobic Ti^{4+} sulfate from Alcaparrosa, Chile

A. R. KAMPF[1,*], S. J. MILLS[2], R. M. HOUSLEY[3], P. A. WILLIAMS[4] AND M. DINI[5]

[1] Mineral Sciences Department, Natural History Museum of Los Angeles County, 900 Exposition Boulevard, Los Angeles, California 90007, USA
[2] Geosciences, Museum Victoria, GPO Box 666, Melbourne 3001, Victoria, Australia
[3] Division of Geological and Planetary Sciences, California Institute of Technology, Pasadena, California 91125, USA
[4] School of Natural Sciences, University of Western Sydney, Locked Bag 1797, Penrith, New South Wales 2751, Australia
[5] Pasaje San Agustin 4045, La Serena, Chile

[*Received 28 September 2011; Accepted 19 December 2011; Associate Editor: G. Diego Gatta*]

ABSTRACT

Alcaparrosaite, ideally $K_3Ti^{4+}Fe^{3+}(SO_4)_4O(H_2O)_2$, is a new mineral from the Alcaparrosa mine, Cerritos Bayos, El Loa Province, Antofagasta, Chile (IMA2011-024). The mineral occurs on and intergrown with coquimbite, and is also associated with ferrinatrite, krausite, pertlikite, pyrite, tamarugite and voltaite. It is a relatively early phase which forms during the oxidation of pyritic masses under increasingly arid conditions. Alcaparrosaite crystallizes from hyperacidic solutions in a chemical environment that is consistent with its association with coquimbite. It occurs as pale yellow blades and tapering prisms up to 4 mm in length, flattened on {010} and elongated along [100]. The observed crystal forms are {010}, {110}, {1.13.0} and {021}. The mineral is transparent and has a white streak, vitreous lustre, Mohs hardness of about 4, brittle tenacity, conchoidal fracture and no cleavage. The measured and calculated densities are 2.80(3) and 2.807 g cm^{-3}, respectively. It is optically biaxial (+) with α = 1.643(1), β = 1.655(1), γ = 1.680(1) (white light), $2V_{meas}$ = 70(2)º and $2V_{calc}$ = 70.3º. The mineral exhibits strong parallel dispersion, $r < v$. The optical orientation is $X = b$; $Y \wedge c = 27º$ in the obtuse angle β. No pleochroism was observed. Electron-microprobe analyses (average of 4) provided: Na_2O 0.32, K_2O 20.44, Fe_2O_3 11.58, TiO_2 11.77, P_2O_5 0.55, SO_3 47.52, H_2O 5.79 (calc); total 97.97 wt.%. The empirical formula (based on 19 O) is $(K_{2.89}Na_{0.07})_{\Sigma 2.96}Ti^{4+}_{0.98}Fe^{3+}_{0.97}(S_{0.99}P_{0.01}O_4)_4O_{0.72}(OH)_{0.28}(H_2O)_2$. The mineral is hydrophobic, insoluble in cold and hot water, very slowly soluble in acids and decomposes slowly in bases. Alcaparrosaite is monoclinic, $C2/c$, with the cell parameters a = 7.55943(14), b = 16.7923(3), c = 12.1783(9) Å, β = 94.076(7)º, V = 1542.01(12) Å^3 and Z = 4. The eight strongest lines in the X-ray powder diffraction pattern [d_{obs} in Å (I_{rel}) (hkl)] are 6.907 (41) (021,110); 3.628 (34) (023,$\bar{1}$13); 3.320 (32) ($\bar{2}$02); 3.096 (100) (202,$\bar{1}$33,150); 3.000 (40) ($\bar{1}$51); 2.704 (38) ($\bar{2}$23,152); 1.9283 (30) ($\bar{1}$55); 1.8406 (31) ($\bar{3}$53,$\bar{2}$06). In the structure of alcaparrosaite (R_1 = 2.57% for 1725 $F_o > 4\sigma F$), Ti^{4+} and Fe^{3+}, in roughly equal amounts, occupy the same octahedrally coordinated site. Octahedra are linked into dimers by corner sharing. The SO_4 tetrahedra link the dimers into chains parallel to [001] and link the chains into undulating sheets parallel to {010}. The sheets link via 10- and 11-coordinated K atoms in the interlayer region. The structure shares some features with that of goldichite.

KEYWORDS: alcaparrosaite, new mineral, hydrous sulfate, crystal structure, hydrophobic, Alcaparrosa mine, Chile.

* E-mail: akampf@nhm.org
DOI: 10.1180/minmag.2012.076.4.03

Introduction

THE new mineral species described herein was first discovered at the Alcaparrosa mine near Cerritos Bayas, Chile (approximately 22º39′S, 69º10′W) in 2008 or 2009 by the German mineral dealer Gunnar Färber; however, the first crystals found were not of adequate size or quality to permit characterization. In 2010 the Chilean mineral collector and dealer Arturo Molina collected crystals of larger size and excellent quality, which he made available for the present study.

The species is named alcaparrosaite for the locality, the Alcaparrosa mine, which is also the type locality for parabutlerite (Bandy, 1938) and paracoquimbite (Ungemach, 1935; Bandy, 1938). It should be noted that another sulfate deposit with the same name is located about 570 km SSE at Tierra Amarilla, near Copiapó, Chile. The new mineral and name have been approved by the Commission on New Minerals, Nomenclature and Classification of the International Mineralogical Association (IMA 2011-024). The description of the new mineral was based upon three specimens, which are designated cotype specimens and are deposited in the Natural History Museum of Los Angeles County, 900 Exposition Boulevard, Los Angeles, CA 90007, USA under catalogue numbers 63519, 63520 and 63521.

Occurrence and paragenesis

The Alcaparrosa mine is located on the west side of Cerro Alcaparrosa, about 3 km southwest of the railway station at Cerritos Bayos, El Loa Province, Antofagasta, Chile. The history, geology and mineralogy of the deposit were described in detail by Bandy (1938).

According to Bandy (1938), the deposit formed by the oxidation of pyritic masses under increasingly arid conditions. Bandy (1938) notes that the sequences of deposition of the minerals are difficult to establish; however, from one inclined pit, he describes a complete series of sulfates from the latest phases at the surface to fresh pyrite at the bottom. A massive layer of coquimbite occurs at a relatively low level and is therefore early in this sequence.

On the cotype specimens, alcaparrosaite occurs on and intergrown with coquimbite and therefore, it is likely to be a relatively early phase at the deposit. It is also associated with ferrinatrite, krausite, pertlikite, pyrite, tamarugite and voltaite. Other minerals that occur at the deposit include aluminocopiapite, amarantite, botryogen, copiapite, cuprocopiapite, fibroferrite, halotrichite, jarosite, krausite, metahohmannite, metavoltine, natrojarosite, parabutlerite, paracoquimbite, pickeringite, quenstedtite, rhomboclase, römerite, sideronatrite and szomolnokite.

Physical and optical properties

Alcaparrosaite crystals occur as blades and tapering prisms up to 4 mm in length (Fig. 1); they are flattened on {010} and elongated along [100]. The observed crystal forms are {010}, {110}, {1.13.0} and {021}. The faces of the {1.13.0} form are typically curved and may actually correspond to several forms, e.g. {190}, {1.11.0} and/or {1.13.0} (Fig. 2). Between crossed polars, some crystals exhibit sectors with slightly different extinction. These could be caused by twinning; however, no twinning was detected during our single-crystal X-ray diffraction study. The commonly tapered aspect of the larger crystals seems more likely to be due to growth factors rather than twinning.

Alcaparrosaite is pale yellow and has a white streak. Crystals are transparent and have vitreous lustre. Alcaparrosaite does not fluoresce in long or

FIG. 1. Alcaparrosaite crystals on coquimbite.

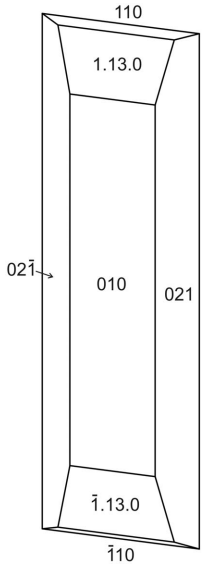

FIG. 2. Alcaparrosaite crystal drawing (clinographic projection in non-standard orientation with [100] vertical).

short wave ultraviolet light. The Mohs hardness is about 4, the tenacity is brittle, the fracture is conchoidal and crystals exhibit no cleavage. The density measured by the sink–float method in an aqueous solution of sodium polytungstate is 2.80(3) g cm^{-3}. The calculated density based on the empirical formula and the unit cell determined by single-crystal X-ray diffraction is 2.807 g cm^{-3}.

Optically, alcaparrosaite is biaxial positive, with α = 1.643(1), β = 1.655(1) and γ = 1.680(1), measured in white light. The 2V measured directly by conoscopic observation is 70(2)º. The calculated 2V is 70.3º. The mineral exhibits strong parallel dispersion, $r < v$. The optical orientation is $X = b$; $Y \wedge c$ = 27º in the obtuse angle β. No pleochroism was observed.

Chemical composition

Four chemical analyses were carried out using a JEOL 8200 electron microprobe at the Division of Geological and Planetary Sciences, California Institute of Technology in wavelength-dispersive spectrometry mode, with an accelerating voltage of 15 kV, a beam current of 5 nA and a 20 μm beam diameter. Quantitative elemental micro-analyses were processed with the CITZAF correction procedure. The standards used were albite (for Na), microcline (for K), pyrite (for Fe), synthetic TiO_2 (for Ti), fluorapatite (for P) and anhydrite (for S).

Insufficient material is available for an accurate direct water determination. A single determination on a 3.7 mg sample using a CEC 440HA CHN analyser in the Marine Science Institute, University of California, Santa Barbara, provided 0.473 wt.% H, equivalent to 4.23 wt.% H_2O. Due to the small sample size and the relatively low water content, this value should be considered to be of low accuracy. Instead, we use the H_2O content of 5.79 wt.% calculated from the structure (based on O = 19 and charge balance).

The averages (and ranges) of the analyses are as follows: Na_2O 0.32 (0.16–0.51), K_2O 20.44 (20.30–20.67), Fe_2O_3 11.58 (11.41–11.71), TiO_2 11.77 (11.54–12.18), P_2O_5 0.55 (0.48–0.68), SO_3 47.52 (46.57–48.06), H_2O 5.79 (calc); total 97.97 wt.%. The empirical formula (based on 19 O) is $(K_{2.89}Na_{0.07})_{\Sigma 2.96}Ti^{4+}_{0.98}Fe^{3+}_{0.97}(S_{0.99}P_{0.01}O_4)_4O_{0.72}(OH)_{0.28}(H_2O)_2$. The simplified formula is $K_3Ti^{4+}Fe^{3+}(SO_4)_4O(H_2O)_2$, which requires K_2O 21.50, TiO_2 12.16, Fe_2O_3, 12.15, SO_3 48.72, H_2O 5.48; total 100.00 wt.%. It is worth noting that OH is provided in the empirical formula merely for charge balance and is not meant to imply the presence of OH in the structure. It is perhaps more realistic to attribute the small stoichiometric deficiencies in (K + Na), Ti and Fe to analytical error.

The Gladstone–Dale compatibility index $1 - (K_P/K_C)$ is −0.001 for the ideal formula and −0.008 for the empirical formula, in both cases indicating superior compatibility (Mandarino, 1981).

For a hydrated sulfate, alcaparrosaite exhibits unusual chemical behaviour. In cold and hot distilled water, it is not only insoluble, but is actually hydrophobic (resists wetting). In concentrated aqueous solutions of HCl (38%), HNO_3 (70%) and H_2SO_4 (96%), crystals are unreactive and dissolve exceedingly slowly; a 0.5 mm crystal fragment requires a day or more to dissolve. In concentrated aqueous solutions of NaOH or KOH, the crystals turn brownish orange and slowly decompose producing a transparent, insoluble residue.

X-ray crystallography and structure refinement

Both powder and single-crystal X-ray studies were carried out using a Rigaku R-Axis Rapid II curved imaging plate microdiffractometer, with

monochromatic Mo$K\alpha$ radiation. For the powder-diffraction study, the observed *d*-spacings and intensities were derived by profile fitting using *JADE 9.3* software. The powder data presented in Table 1 are in good agreement with the pattern calculated from the structure determination. The unit-cell parameters refined from the powder data using *JADE 9.3* with whole pattern fitting are a = 7.577(6), b = 16.815(6), c = 12.208(6) Å, β = 94.116(11)º and V = 1551.5(15) Å^3.

The Rigaku *CrystalClear* software package was used for processing the structure data, including the application of an empirical absorption correction. The systematic absences are consistent with the space groups *C*2, *Cm* and *C*2/*m* and the E-statistics (Sheldrick, 2008) suggest the structure to be centrosymmetric and therefore in space group *C*2/*m*. The structure was solved by direct methods using *SIR2004* (Burla *et al*., 2005) and refined with *SHELXL-97* (Sheldrick, 2008). Two H atoms of the H_2O group were located in the difference-Fourier map. The Fe and Ti were jointly refined at the octahedral *M* site, providing occupancies of Fe 0.432(10) and Ti 0.568(10); however, in the final refinement the *M* site was assigned an occupancy of ½ Fe and ½ Ti, as indicated by the chemical analysis. The small amount of Na in the chemical analysis probably occupies the K1 and K2 sites, as suggested by the smaller average bond lengths and higher bond-valence sums for those sites compared to the K3 site. Nevertheless, because the amount of Na was so small, all three sites were assigned full occupancy by K in the final refinement.

The details of the data collection and the final structure refinement are provided in Table 2. The

TABLE 1. Powder X-ray diffraction data for alcaparrosaite.

I_{obs}	d_{obs}	d_{calc}	I_{calc}	$h\ k\ l$	I_{obs}	d_{obs}	d_{calc}	I_{calc}	$h\ k\ l$	I_{obs}	d_{obs}	d_{calc}	I_{calc}	$h\ k\ l$
3	8.408	8.3962	6	0 2 0	7	2.4836	2.4968	4	2 4 2	10	1.6375	1.6429	3	1 9 3
41	6.907	6.9069	57	0 2 1			2.4857	2	3 1 0			1.6404	4	0 6 6
		6.8787	14	1 1 0			2.4696	4	$\bar{3}$ 1 1			1.6352	7	3 5 4
13	6.169	6.1593	12	$\bar{1}$ 1 1	13	2.4116	2.4120	35	1 5 3	3	1.5918	1.6019	3	2 4 6
2	5.832	5.8258	4	1 1 1	12	2.3504	2.3651	2	$\bar{2}$ 4 3			1.5883	3	0 8 5
21	4.929	4.9211	38	0 2 2			2.3534	5	$\bar{2}$ 2 4	8	1.5656	1.5674	5	3 7 3
24	4.723	4.7068	26	$\bar{1}$ 1 2			2.3338	4	0 2 5			1.5529	6	4 0 4
4	4.143	4.1582	3	1 3 1	15	2.2471	2.2472	9	2 6 0			1.5274	3	$\bar{2}$ 10 1
		3.6883	11	$\bar{1}$ 3 2			2.2459	4	3 1 2	17	1.5180	1.5184	12	0 0 8
34	3.628	3.6472	15	0 2 3			2.2455	7	1 1 5	4	1.4932	1.5082	5	3 5 5
		3.5928	26	$\bar{1}$ 1 3	8	2.2116	2.2267	5	$\bar{2}$ 6 1			1.4976	3	$\bar{2}$ 10 2
		3.4534	5	0 4 2			2.2066	6	2 2 4			1.4921	6	1 5 7
20	3.438	3.4393	19	2 2 0	7	2.1001	2.1003	6	1 3 5	8	1.4731	1.4793	4	3 9 1
		3.3670	8	$\bar{2}$ 2 1			2.0990	5	0 8 0			1.4697	6	$\bar{3}$ 5 6
32	3.320	3.3104	31	$\bar{2}$ 0 2	2	2.0526	2.0684	4	0 8 1	8	1.4471	1.4484	6	$\bar{2}$ 10 3
		3.2544	6	2 2 1			2.0550	2	3 1 3			1.4461	3	$\bar{3}$ 7 5
100	3.096	3.1058	100	2 0 2			2.0531	2	$\bar{3}$ 3 3	7	1.4249	1.4248	5	$\bar{3}$ 9 3
		3.0738	40	$\bar{1}$ 3 3	6	2.0102	2.0093	12	$\bar{1}$ 7 3	8	1.3777	1.3814	3	0 10 5
		3.0679	46	1 5 0			1.9673	10	3 5 1			1.3770	3	$\bar{5}$ 5 1
		3.0369	28	0 0 4			1.9419	6	3 3 3			1.3768	4	$\bar{1}$ 5 8
40	3.000	2.9951	52	$\bar{1}$ 5 1	30	1.9283	1.9320	20	$\bar{1}$ 5 5	13	1.3556	1.3609	3	$\bar{5}$ 5 2
		2.9543	6	1 5 1	3	1.8786	1.8851	5	4 0 0			1.3535	4	2 10 4
25	2.848	2.8472	20	$\bar{1}$ 1 4			1.8785	6	3 5 2			1.3528	3	$\bar{3}$ 5 7
		2.7708	7	$\bar{1}$ 5 2	31	1.8406	1.8444	10	$\bar{3}$ 5 3	7	1.2809	1.2848	4	$\bar{5}$ 5 4
		2.7654	7	$\bar{2}$ 4 1			1.8390	12	$\bar{2}$ 0 6			1.2804	5	2 10 5
		2.7273	6	0 6 1	22	1.7213	1.7232	5	$\bar{3}$ 5 4			1.2776	3	5 5 3
38	2.704	2.7095	16	$\bar{2}$ 2 3			1.7197	18	4 4 0			1.2533	3	$\bar{4}$ 10 1
		2.7071	30	1 5 2			1.7127	5	$\bar{1}$ 5 6	19	1.2497	1.2517	3	3 9 5
20	2.609	2.5994	31	$\bar{2}$ 4 2	9	1.6780	1.6927	2	$\bar{2}$ 8 3			1.2484	6	$\bar{6}$ 0 2
		2.5673	4	$\bar{1}$ 3 4			1.6876	2	4 4 1	10	1.2151	1.2237	2	5 5 4
							1.6857	2	$\bar{2}$ 6 5			1.2137	3	6 0 2
							1.6845	2	$\bar{2}$ 4 6	6	1.1802	1.1810	2	$\bar{2}$ 0 10
												1.1767	3	$\bar{4}$ 4 8

TABLE 2. Data collection and structure refinement details for alcaparrosaite.

Diffractometer	Rigaku R-Axis Rapid II
X-ray radiation / power	Mo$K\alpha$ (λ = 0.71075 Å) / 50 kV, 40 mA
Temperature	298(2) K
Structural Formula	$K_3Ti^{4+}Fe^{3+}(SO_4)_4O(H_2O)_2$
Space group	$C2/c$
Unit cell dimensions	a = 7.55943(14) Å
	b = 16.7923(3) Å
	c = 12.1783(9) Å
	β = 94.076(7)°
V	1542.01(12) Å^3
Z	4
Density (for above formula)	2.831 g cm^{-3}
Absorption coefficient	2.918 mm^{-1}
F(000)	1300
Crystal size	220 × 210 × 70 μm
θ range	3.31 to 27.46°
Index ranges	$-9 \leqslant h \leqslant 9$, $-21 \leqslant k \leqslant 21$, $-15 \leqslant l \leqslant 15$
Reflections collected / unique	16,494 / 1756 [R_{int} = 0.0202]
Reflections with $F_o > 4\sigma F$	1726
Completeness to θ = 27.46°	99.6%
Max. and min. transmission	0.8218 and 0.5662
Refinement method	Full-matrix least-squares on F^2
Parameters refined	140
GoF	1.198
Final R indices [$F_o > 4\sigma F$]	R_1 = 0.0263, wR_2 = 0.0674
R indices (all data)	R_1 = 0.0267, wR_2 = 0.0676
Largest diff. peak / hole	+0.55 / −0.53 e$^-$ A^{-3}

$R_{int} = \Sigma|F_o^2 - F_o^2(\text{mean})|/\Sigma[F_o^2]$.
GoF = $S = \{S[w(F_o^2 - F_c^2)^2]/(n-p)\}^{1/2}$.
$R_1 = \Sigma||F_o| - |F_c||/\Sigma|F_o|$. $wR_2 = \{\Sigma[w(F_o^2 - F_c^2)^2]/\Sigma[w(F_o^2)^2]\}^{1/2}$.
$w = 1/[\sigma^2(F_o^2) + (aP)^2 + bP]$ where a is 0.0364, b is 2.7570 and P is $[2F_c^2 + \text{Max}(F_o^2,0)]/3$.

final atomic coordinates and displacement parameters are provided in Table 3. Selected interatomic distances are listed in Table 4 and bond valences in Table 5. Lists of observed and calculated structure factors have been deposited with *Mineralogical Magazine* and are available at www.minersoc.org/pages/e_journals/dep_mat.html.

Description of the structure

In the structure of alcaparrosaite (Fig. 3), Ti^{4+} and Fe^{3+}, in roughly equal amounts, occupy the same octahedrally coordinated site (*M*). One octahedral vertex (O9) is shared between two octahedra, producing a corner-sharing dimer. The opposite (*trans*) vertex (OW) is an H_2O group and the four remaining vertices (O3, O4, O6 and O8), around the girdle of each octahedron, are shared with SO_4 tetrahedra. The S3 tetrahedron forms an additional link between the octahedra of the dimer by sharing their O8 vertices, resulting in the combined linkage (described hereafter as a cluster) shown in Fig. 4*a*. Pairs of S1 tetrahedra form a double link between the octahedra of adjacent dimers by sharing O3 and O4 vertices, resulting in the cluster shown in Fig. 4*b*. The combination of the linkages illustrated in Fig. 4*a* and *b* produces chains of octahedra and tetrahedra parallel to [001]. The S2 tetrahedron links octahedra in adjacent chains by sharing O6 vertices, resulting in the cluster shown in Fig. 4*c*. The combination of the linkages in Fig. 4*a*–*c* yields the sheet parallel to {010} shown in Fig. 3*b*. Bonding between the sheets is via three different K atoms in the interlayer region (see Fig. 3*a*); K1 and K2 are 10-coordinated and K3 is 11-coordinated.

TABLE 3. Atomic coordinates and displacement parameters (Å^2) for alcaparrosaite.

Site	*x*/*a*	*y*/*b*	*z*/*c*	U_{eq}	U_{11}	U_{22}	U_{33}	U_{23}	U_{13}	U_{12}
K1	0.0000	0.47481(4)	0.7500	0.01896(15)	0.0162(3)	0.0150(3)	0.0251(3)	0.000	−0.0021(2)	0.000
K2	0.2500	0.7500	0.5000	0.01914(14)	0.0176(3)	0.0207(3)	0.0189(3)	0.0020(2)	−0.0002(2)	0.0017(2)
K3	0.5000	0.39010(4)	0.7500	0.0372(2)	0.0267(4)	0.0212(4)	0.0646(6)	0.000	0.0101(4)	0.000
*M**	0.61968(4)	0.610717(17)	0.63562(2)	0.01168(11)	0.01078(16)	0.01044(17)	0.01344(17)	−0.00212(10)	−0.00181(11)	0.00056(10)
S1	0.26049(6)	0.53961(3)	0.50891(4)	0.01092(12)	0.0094(2)	0.0116(2)	0.0117(2)	−0.00246(15)	0.00044(15)	−0.00037(15)
S2	0.0000	0.68381(4)	0.7500	0.01056(14)	0.0080(3)	0.0108(3)	0.0127(3)	0.000	−0.0011(2)	0.000
S3	0.5000	0.77535(4)	0.7500	0.01101(14)	0.0115(3)	0.0083(3)	0.0131(3)	0.000	0.0002(2)	0.000
O1	0.10172(19)	0.58733(9)	0.49537(13)	0.0216(3)	0.0131(7)	0.0225(7)	0.0290(8)	−0.0054(6)	0.0005(6)	0.0047(6)
O2	0.2635(2)	0.48252(9)	0.59862(11)	0.0187(3)	0.0231(7)	0.0185(7)	0.0145(7)	0.0012(5)	0.0021(5)	−0.0043(5)
O3	0.41890(18)	0.59460(8)	0.52202(11)	0.0147(3)	0.0134(6)	0.0154(6)	0.0149(6)	−0.0004(5)	−0.0022(5)	−0.0038(5)
O4	0.71700(18)	0.50419(8)	0.59826(11)	0.0146(3)	0.0180(6)	0.0131(6)	0.0123(6)	−0.0033(5)	−0.0011(5)	0.0020(5)
O5	1.00753(19)	0.73230(9)	0.65145(12)	0.0187(3)	0.0182(7)	0.0197(7)	0.0181(7)	0.0062(5)	−0.0001(5)	−0.0028(5)
O6	0.84151(17)	0.62944(9)	0.73680(11)	0.0157(3)	0.0122(6)	0.0164(6)	0.0181(7)	0.0022(5)	−0.0031(5)	−0.0042(5)
O7	0.65673(19)	0.82283(9)	0.77721(12)	0.0195(3)	0.0162(7)	0.0162(7)	0.0257(7)	−0.0015(6)	−0.0007(6)	−0.0052(5)
O8	0.53144(19)	0.72169(8)	0.65363(11)	0.0166(3)	0.0234(7)	0.0119(6)	0.0144(6)	−0.0009(5)	0.0014(5)	0.0024(5)
O9	0.5000	0.57331(11)	0.7500	0.0131(4)	0.0132(8)	0.0131(9)	0.0130(8)	0.000	0.0009(7)	0.000
OW	0.75575(19)	0.66205(9)	0.50808(12)	0.0166(3)	0.0173(7)	0.0167(7)	0.0160(7)	0.0001(5)	0.0033(5)	−0.0021(5)
H1	0.794(7)	0.630(3)	0.459(4)	0.12(2)						
H2	0.825(5)	0.6985(19)	0.533(3)	0.070(13)						

* The *M* site was assigned ½ Ti and ½ Fe.

TABLE 4. Selected bond distances (Å) and angles (°) in alcaparrosaite.

K1–O4 (×2)	2.7700(13)	K2–O5 (×2)	2.7075(14)	K3–O7 (×2)	2.8709(14)
K1–O2 (×2)	2.8114(14)	K2–O8 (×2)	2.7725(14)	K3–O5 (×2)	2.9111(17)
K1–O7 (×2)	2.8234(16)	K2–O3 (×2)	2.9091(14)	K3–O2 (×2)	2.9216(15)
K1–O6 (×2)	2.8594(15)	K2–O1 (×2)	2.9517(16)	K3–O9	3.0765(21)
K1–O1 (×2)	3.2066(16)	K2–O7 (×2)	3.0136(15)	K3–O4 (×2)	3.1948(15)
<K–O>	**2.8942**	**<K–O>**	**2.8709**	K3–O3 (×2)	3.4212(14)
				<K–O>	**3.0651**
M–O9	1.8255(7)	S1–O1	1.4429(15)	S2–O5 (×2)	1.4548(14)
M–O8	1.9966(14)	S1–O2	1.4524(15)	S2–O6 (×2)	1.5058(14)
M–O3	1.9981(14)	S1–O3	1.5117(14)	**<S–O>**	**1.4803**
M–O4	1.9990(14)	S1–O4	1.5181(13)		
M–O6	2.0335(14)	**<S–O>**	**1.4813**	S3–O7 (×2)	1.4468(14)
M–OW	2.1073(14)			S3–O8 (×2)	1.5117(14)
<*M*–O>	**2.0269**			**<S–O>**	**1.4793**

Hydrogen bonds (D = donor, A = acceptor)

D–H	*d*(D–H)	*d*(H···A)	<DHA	*d*(D···A)	A	<HDH
OW–H1	0.87(2)	2.06(4)	137(5)	2.752(2)	O2	118(3)
OW–H2	0.85(2)	2.00(3)	147(4)	2.755(2)	O5	

The structure of alcaparrosaite has no analogues. The sheet and chain topologies in the structure are unique. The alcaparrosaite structure is related to the sulfate minerals having an infinite, non-brucite-like sheet of octahedra and tetrahedra in the structural hierarchy of sulfate minerals proposed by Hawthorne *et al*. (2000). However, no sulfate mineral structure possesses a sheet similar to that in alcaparrosaite and although Hawthorne *et al*. (2000) note structures with chains composed entirely the cluster depicted in Fig. 4*a* (e.g. fibroferrite) and entirely of that depicted in Fig. 4*b* (e.g. butlerite), they do not note any structure composed of a combination of those two clusters.

The octahedral cation in the structure of alcaparrosaite has an ideal effective charge of 3.5+. The structural hierarchy of Hawthorne *et al*. (2000) does not describe octahedral cations with charges greater than 3+, as they were not known at that time in minerals, although the structures of the synthetic compounds $Ti^{4+}OSO_4$ and $Ti^{4+}OSO_4 \cdot H_2O$ had been described by Gatehouse *et al*. (1993). These two structures do not resemble that of alcaparrosaite in their general structural motif and their local octahedral–tetrahedral linkages are also not very similar to those in alcaparrosaite.

Undulating sheets of $Fe^{3+}O_6$ octahedra and SO_4 tetrahedra are also found in the structure of goldichite, $KFe^{3+}(SO_4)_2(H_2O)_4$ (Graeber and Rosenzweig, 1971). The structures share some similar features, including the general shape of their undulating sheets, the linkages between octahedra and tetrahedra shown in Fig. 4*b*,c (but not 4*a*) and K atoms in the interlayer region; however, the goldichite structure does not contain any shared octahedral corners. The two structures are compared in Fig. 3.

Paragenesis

The remarkably dry climate of northern Chile is, in the words of Bandy (1938):

"...exceptionally favorable for the formation of sulfates, chlorides and oxides from concentrated solutions and from solutions that maintain a uniform composition over long periods of time ... The water table is far below the surface and the primary sulfide horizon ... Rains capable of adding an appreciable amount of water to the deposit, that is, a sufficient amount to even moisten the entire oxide zone, only occur once in a decade as a rule. During the intervening periods the sulfates form from concentrated solutions and then, once formed, change very slowly. There can be no question but that many of the sulfates form from older sulfates through reactions taking place in moist air and not by precipitation from aqueous solutions."

The stability of alcaparrosaite in water and its very slow solubility in concentrated acids is rather

TABLE 5. Bond-valence analysis for alcaparrosaite. Values are expressed in valence units.

	O1	O2	O3	O4	O5	O6	O7	O8	O9	OW	Σ
K1	0.052 ×2→	0.151 ×2→		0.169×2→		0.133 ×2→	0.147 ×2→				1.304
K2	0.104 ×2→		0.116 ×2→		0.201 ×2→		0.088 ×2→	0.168 ×2→			1.354
K3		0.112 ×2→	0.029 ×2→	0.054 ×2→	0.116 ×2→		0.129 ×2→		0.074		0.954
M			0.567	0.565		0.515		0.569	0.904 ×2↓	0.422	3.542
S1	1.631	1.590	1.355	1.331							5.906
S2					1.580 ×2→	1.376 ×2→					5.911
S3							1.614 ×2→	1.355 ×2→			5.936
H1		0.110								0.890	1.000
H2					0.125					0.875	1.000
Σ	1.787	1.963	2.067	2.119	2.022	2.024	1.978	2.092	1.882	2.187	

Multiplicity is indicated by × →↓; Fe^{3+}–O, Ti^{4+}–O and S^{6+}–O bond strengths are from Brown and Altermatt (1985); the K–O bond strength is from Wood and Palenik (1999); hydrogen-bond strengths are based on H···O bond lengths, also from Brown and Altermatt (1985).

enigmatic, as it is the only phase in the assemblage for which this is the case. Its hydrophobic behaviour is also unusual. The resistance of hydrophobic materials to wetting results from their reluctance to form hydrogen bonds to H_2O molecules at the crystal–water interface. It is not immediately obvious from an examination of the alcaparrosaite structure why this should be the case. As noted above, goldichite has chemical and structural similarities to alcaparrosaite. It also appears to exhibit hydrophobic behaviour, but is slightly soluble in cold water, soluble in hot water and readily soluble in acids. It exhibits similar reactivity with bases as alcaparrosaite. The fact that alcaparrosaite is the only Ti-bearing phase reported from the Alcaparrosa deposit is also noteworthy. An EDS survey of all the minerals associated with alcaparrosaite did not reveal any other phases that contained detectable Ti.

The mineralogy of the Alcaparrosa deposit (Bandy, 1938) reflects the deposition of a series of Fe^{2+}–Fe^{3+} sulfates in a number of microenvironments, some of which were hyperacidic. In this connection, the intimate association of alcaparrosaite with coquimbite is a key observation. The general sequence of crystallization of Fe^{2+}–Fe^{3+} with increasing acidity between 30 and 40ºC is goethite → hydronium jarosite → butlerite → ferricopiapite → coquimbite → kornelite → rhomboclase (Merwin and Posnjak, 1937). Phase relationships in the system Fe_2O_3–SO_3–H_2O have been established for more than 70 years (Cameron and Robinson, 1907; Wirth and Bakke, 1914; Appleby and Wilkes, 1922; Posnjak and Merwin, 1922; Baskerville and Cameron, 1935; Merwin and Posnjak, 1937), and have stood the test of time. As far as coquimbite, $Fe_2(SO_4)_3{\cdot}9H_2O$, and kornelite, $Fe_2(SO_4)_3{\cdot}7H_2O$, are concerned, the latter occupies a very narrow range of conditions in the ternary system at 30 to 40ºC (Merwin and Posnjak, 1937). Sulfuric acid concentrations that span the stability fields of ferricopiapite, coquimbite and rhomboclase are approximately 2 to 5 mol kg^{-1}. Conditions under which coquimbite is stable can be expressed alternatively in terms of equilibrium considerations, as described below.

Majzlan *et al.* (2006) reported $\Delta G_f^{\ominus}$(298.2 K) data for ferricopiapite, $Fe_{4.78}(SO_4)_6(OH)_{2.34}(H_2O)_{20.71}$, and rhomboclase, $(H_3O)_{1.34}Fe(SO_4)_{2.17}(H_2O)_{3.06}$, as −10,089.8±9.3 and −2688.0±2.7 kJ mol^{-1}, respectively. As far as coquimbite is concerned, it is noted that the

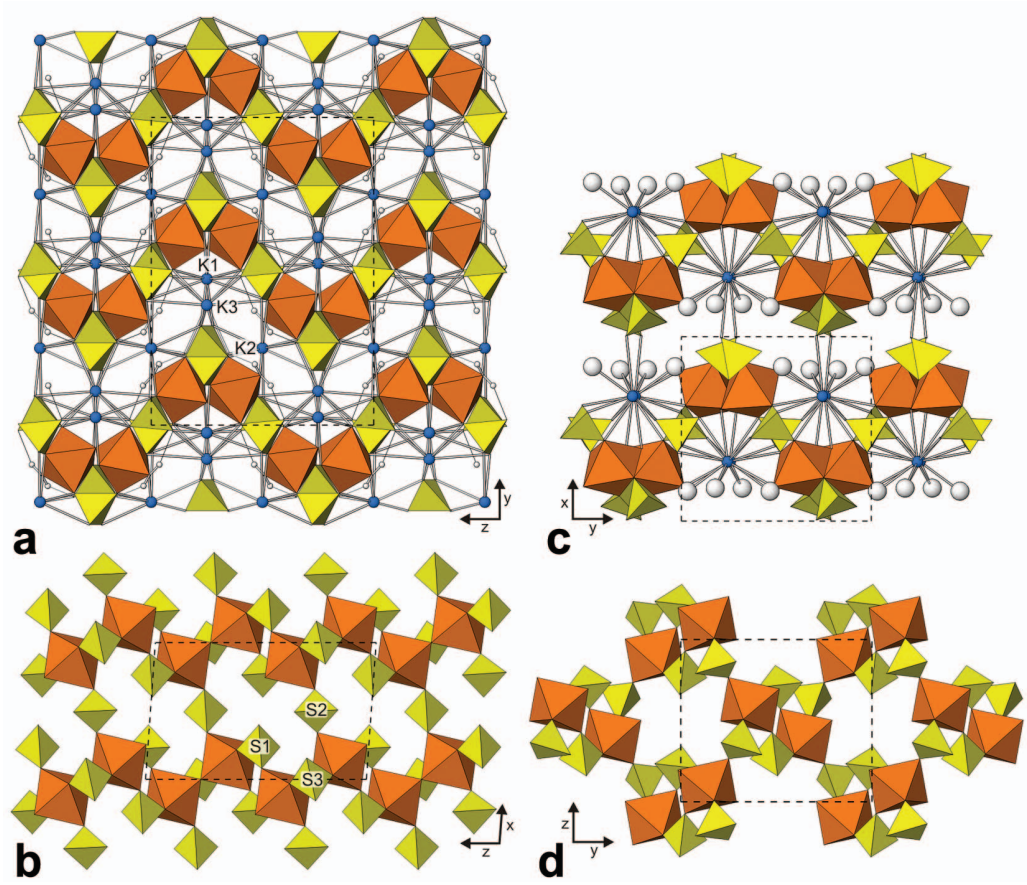

FIG. 3. The structures of (*a*,*b*) alcaparrosaite and (*c*,*d*) goldichite. The structures shown in (*a*) and (*c*) include all components and show the undulating shapes of the sheets. The structures shown in (*b*) and (*d*) show only the octahedra and tetrahedra in a single sheet. The MO_6 octahedra (M = Fe^{3+},Ti^{4+} in alcaparrosaite and Fe^{3+} in goldichite) are orange; SO_4 tetrahedra are yellow; K atoms are blue spheres; H atoms are small white spheres; H_2O groups in goldichite are large white spheres.

estimated value for $\Delta G_f^{\ominus}$ (coquimbite, 298.2K) of -4250.6 kJ mol^{-1} given by Hemingway *et al.* (2002) is incompatible with the experimentally determined quantity for ferricopiapite. However, Majzlan *et al.* (2006) also reported thermochemical data for a sample of natural coquimbite of composition $Fe_{1.47}Al_{0.43}(SO_4)_3{\cdot}9.65H_2O$. Assuming that the enthalpy of dissolution of $Fe_3(SO_4)_3{\cdot}9.65H_2O$ is the same as that of $Fe_{1.47}Al_{0.43}(SO_4)_3{\cdot}9.65H_2O$, and using the same Hess cycle as Majzlan *et al.* (2006), $\Delta H_f^{\ominus}$(298.2K) of $Fe_3(SO_4)_3{\cdot}9.65H_2O$ is -5474.4 kJ mol^{-1}. Similarly, the method of Majzlan *et al.* (2006) gives S^{o}(298.2 K,$Fe_3(SO_4)_3{\cdot}9.65H_2O$, s) = +655.9 J K^{-1} mol^{-1} and $\Delta G_f^{\ominus}$(298.2K) is then equal to -4586.2 kJ mol^{-1}. The following may then be calculated, using the thermochemical data of Cox *et al.* (1989) for SO_4^{2-}(aq) and H_2O(l).

$$2Fe_{4.78}(SO_4)_6(OH)_{2.34}(H_2O)_{20.71} + 2.34HSO_4^- + 2.34H^+ + 0.027H_2O \rightleftharpoons 4.78Fe_2(SO_4)_3{\cdot}9.65H_2O$$
$$pH = -2.36 + \lg a(HSO_4^-) + 0.012 \lg a(H_2O)$$

$$Fe_2(SO_4)_3{\cdot}9.65H_2O + 1.34HSO_4^- + 1.34H^+ \rightleftharpoons 2(H_3O)_{1.34}Fe(SO_4)_{2.17}(H_2O)_{3.06} + 0.85H_2O$$
$$pH = -2.72 - 0.634 \lg a(H_2O) + \lg a(HSO_4^-)$$

These boundary conditions include $a(H_2O)$ and this is approximately 0.85 for the sulfuric acid solutions involved (Robertson and Dunford, 1964). The conditions are geochemically sensible,

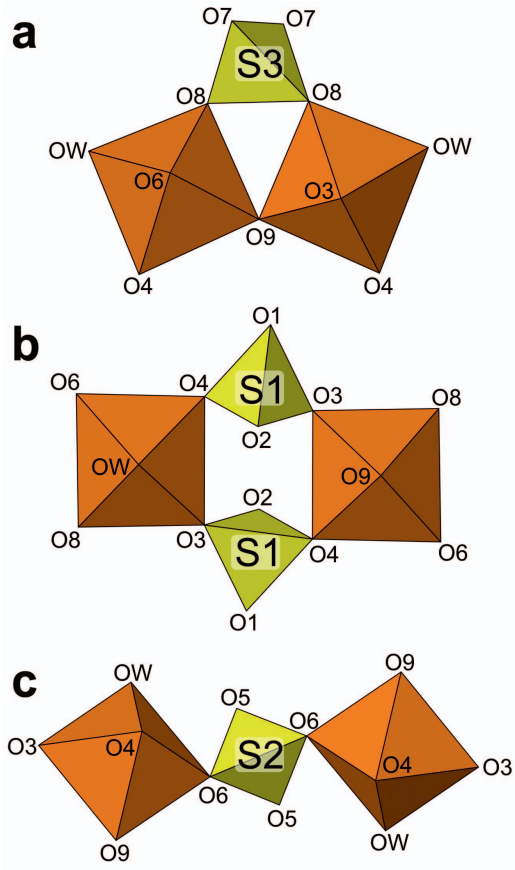

FIG. 4. Three types of octahedral–tetrahedral clusters in the structure of alcaparrosaite: (*a*) an octahedral dimer with additional linking tetrahedron, (*b*) a double tetrahedral linkage between octahedra, and (*c*) a single tetrahedral link between octahedra. The linkages shown in (*b*) and (*c*) are also found in the structure of goldichite. The atom labels apply only to alcaparrosaite.

giving rise to a stability field for coquimbite between those of ferricopiapite and rhomboclase, and they are completely consistent with the observations of Merwin and Posnjak (1937) with respect to the concentrations of sulfuric acid that are needed to stabilize coquimbite at ambient temperatures.

The question that remains is how this relates to Ti^{4+} and its incorporation in the alcaparrosaite lattice. Titanium dioxide is insoluble in H_2SO_4, but ilmenite dissolves in strongly acidic solutions to yield solutions containing titanyl sulfate, $TiOSO_4$. In such solutions, the main dissolved Ti(VI) species are $Ti(OH)_2^{2+}$(aq) and TiO^{2+}(aq) (Baes and Mesmer, 1976), and the titanyl sulfate complexes $TiOSO_4^0$(aq) and $TiO(SO_4)_2^{2-}$(aq) (Szilágyi *et al*., 2009*a*). This is the basis of the so-called 'sulfate process' for making TiO_2 from ilmenite and Ti-rich slags (e.g. Mackey, 1974). Appreciable amounts of Ti^{4+} remain in solution at sulfuric acid concentrations comparable to those associated with the crystallization of coquimbite (Grzmil *et al*., 2008). The $[TiOFe(SO_4)_3]^{2-}$ complex is stable in strong acid and may be oxidized to its Fe^{3+} congener (Szilágyi *et al*., 2009*b*). Such species may be the solution precursors to the nucleation of alcaparrosaite. Thus it is sulfuric acid generated by the oxidation of pyrite, and concentrated by evaporation, that has broken down Ti-bearing gangue minerals and is responsible for concentrating sufficient Ti^{4+} in solution to give rise to the formation of alcaparrosaite. Just what the original Ti minerals were is not known.

Acknowledgements

Reviewers Elena Sokolova and Fernando Cámara are thanked for their constructive comments on the manuscript. Arturo Molina is thanked for providing the specimens of alcaparrosaite. The EMP analyses were supported by a grant to the California Institute of Technology from the Northern California Mineralogical Association. The remainder of this study was funded by the John Jago Trelawney Endowment to the Mineral Sciences Department of the Natural History Museum of Los Angeles County.

References

Appleby, M.P. and Wilkes, S.H. (1922) The system ferric oxide-sulphuric acid-water. *Journal of the Chemical Society*, **121**, 337–348.

Baes, C.F. Jr and Mesmer, R.E. (1976) *The Hydrolysis of Cations*. Wiley and Sons, New York.

Bandy, M.C. (1938) Mineralogy of three sulfate deposits of northern Chile. *American Mineralogist*, **23**, 669–760.

Baskerville, W.H. and Cameron, F.K. (1935) Ferric oxide and aqueous sulfuric acid at 25ºC. *Journal of Physical Chemistry*, **39**, 769–779.

Brown, I.D. and Altermatt, D. (1985) Bond-valence parameters from a systematic analysis of the inorganic crystal structure database. *Acta Crystallographica*, **B41**, 244–247.

Burla, M.C., Caliandro, R., Camalli, M., Carrozzini, B., Cascarano, G.L., De Caro, L., Giacovazzo, C.,

Polidori, G. and Spagna, R. (2005) *SIR2004*: an improved tool for crystal structure determination and refinement. *Journal of Applied Crystallography*, **38**, 381–388.

Cameron, F.K. and Robinson, C. (1907) Ferric sulfates. *Journal of Physical Chemistry*, **11**, 641–650.

Cox, J.D., Wagman, D.D. and Medvedev, V.A. (1989) *CODATA Key Values for Thermodynamics*. Hemisphere Publishing Corporation, New York.

Gatehouse, B.M., Platts, S.N and Williams, T.B. (1993) Structure of anhydrous titanyl sulfate, titanyl sulfate monohydrate and prediction of a new structure. *Acta Crystallographica*, **B49**, 428–435.

Graeber, E.J. and Rosenzweig, A. (1971) The crystal structures of yavapaiite, $KFe(SO_4)_2$, and goldichite, $KFe(SO_4)_2{\cdot}4H_2O$. *American Mineralogist*, **56**, 1917–1933

Grzmil, B.U., Grela, D. and Kic, B. (2008) Hydrolysis of titanium sulphate compounds. *Chemical Papers*, **62**, 18–25.

Hawthorne, F.C., Krivovichev, S.V. and Burns, P.C. (2000) The crystal chemistry of sulfate minerals. Pp. 1–112 in: *Sulfate Minerals – Crystallography, Geochemistry, and Environmental Significance*. Reviews in Mineralogy & Geochemistry, **40**. Mineralogical Society of America, Washington D.C.

Hemingway, B.S., Seal, R.R. and Chou, I.-M. (2002) Thermodynamic data for modelling acid mine drainage problems: compilation and estimation of data for selected soluble iron-sulfate minerals. *United States Geological Survey Open-File Report*, 02–161.

Mackey, T.S. (1974) Acid leaching of ilmenite into synthetic rutile. *Industrial and Engineering Chemistry Product Research and Development*, **13**, 9–17.

Majzlan, J., Navrotsky, A., McCleskey, R.B. and Alpers, C.N. (2006) Thermodynamic properties and crystal structure refinement of ferricopiapite, coquimbite, rhomboclase and $Fe_2(SO_4)_3(H_2O)_5$. *European Journal of Mineralogy*, **18**, 175–186.

Mandarino, J.A. (1981) The Gladstone–Dale relationship: part IV. The compatibility concept and its application. *The Canadian Mineralogist*, **19**, 441–450.

Merwin, H.E. and Posnjak, E. (1937) Sulfate incrustations in the Copper Queen mine, Bisbee, Arizona. *American Mineralogist*, **22**, 567–571.

Posnjak, E. and Merwin, H.E. (1922) The system, $Fe_2O_3–SO_3–H_2O$. *Journal of the American Chemical Society*, **44**, 1965–1994.

Robertson, E.B. and Dunford, H.B. (1964) The state of the proton in aqueous sulfuric acid. *Journal of the American Chemical Society*, **86**, 5080–5089.

Sheldrick, G.M. (2008) A short history of *SHELX*. *Acta Crystallographica*, **A64**, 112–122.

Szilágyi, I., Königsberger, E. and May, P.M. (2009*a*) Spectroscopic characterization of weak interactions in acidic titanyl sulfate solutions for production of titanium dioxide precipitates. *Inorganic Chemistry*, **48**, 2200–2204.

Szilágyi, I., Königsberger, E. and May, P.M. (2009*b*) Characterization of chemical speciation of titanyl sulfate-iron(II) sulfate solutions. *Journal of the Chemical Society*, *Dalton Transactions*, **2009**, 7717–7724.

Ungemach, P. (1935) Sur certains minéraux sulfatés du Chili. *Bulletin de la Société française de Minéralogie*, **58**, 97–221.

Wirth, F. and Bakke, B. (1914) Untersuchung über Ferrisulfate. Darstellung und Eigenschaften der verschiedenen normalen, basischen und sauren Ferrisulfate. Löslichkeits- und Stabilitätsverhältnisse in Wasser und Schwefelsäure. Kristallisationsgang. *Zeitschrift für anorganische Chemie*, **87**, 13–46.

Wood, R.M. and Palenik, G.J. (1999) Bond valence sums in coordination chemistry using new R_0 values. Potassium–oxygen complexes. *Inorganic Chemistry*, **38**, 1031–1034.